Title
Estimation of coronary artery hyperemic blood flow based on arterial lumen volume using angiographic images

Journal
The International Journal of Cardiovascular Imaging, 28(1)

ISSN
1569-5794

Authors
Molloi, Sabee
Chalyan, David
Le, Huy
et al.

Publication Date
2012

DOI
10.1007/s10554-010-9766-1

Int J Cardiovasc Imaging (2012) 28:1–11
DOI 10.1007/s10554-010-9766-1

ORIGINAL PAPER

Estimation of coronary artery hyperemic blood flow based on arterial lumen volume using angiographic images

Sabee Molloi · David Chalyan · Huy Le · Jerry T. Wong

Received: 19 March 2010 / Accepted: 7 December 2010 / Published online: 7 January 2011

Abstract The purpose of this study is to develop a method to estimate the hyperemic blood flow in a coronary artery using the sum of the distal lumen volumes in a swine animal model. The limitations of visually assessing coronary artery disease are well known. These limitations are particularly important in intermediate coronary lesions where it is difficult to determine whether a particular lesion is the cause of ischemia. Therefore, a functional measure of stenosis severity is needed using angiographic image data. Coronary arteriography was performed in 10 swine (Yorkshire, 25–35 kg) after power injection of contrast material into the left main coronary artery. A densitometry technique was used to quantify regional flow and lumen volume in vivo after inducing hyperemia. Additionally, 3 swine hearts were casted and imaged post-mortem using cone-beam CT to obtain the lumen volume and the arterial length of corresponding coronary arteries. Using densitometry, the results showed that the stem hyperemic flow (Q) and the associated crown lumen volume (V) were related by $Q = 159.08\ V^{3/4}$ ($r = 0.98$, $SEE = 10.59$ ml/min). The stem hyperemic flow and the associated crown length (L) using cone-beam CT were related by $Q = 2.89\ L$ ($r = 0.99$, $SEE = 8.72$ ml/min). These results indicate that measured arterial branch lengths or lumen volumes can potentially be used to predict the expected hyperemic flow in an arterial tree. This, in conjunction with measured hyperemic flow in the presence of a stenosis, could be used to predict fractional flow reserve based entirely on angiographic data.

Keywords Angiography · Blood flow · Blood volume · Regional blood flow · Stenosis

S. Molloi (✉) · D. Chalyan · H. Le · J. T. Wong
Department of Radiological Sciences,
University of California, Medical Sciences B, B-140,
Irvine, CA 92697, USA
e-mail: symolloi@uci.edu

Introduction

Subjective visual grading of the severity of coronary artery stenosis by angiography is highly variable, correlating poorly with blood flow and ischemic potential. Several studies have documented the large intraobserver and interobserver variability that results from subjective visual grading of coronary stenotic lesions [1–3]. Angiography alone cannot fully characterize the clinical significance of coronary stenosis. This is particularly important in the case of an intermediate coronary lesion (30–70% diameter stenosis), where coronary arteriography is very limited in distinguishing whether a lesion is ischemia producing. A functional measure of the coronary stenosis severity, such as hyperemic blood flow normalized to the associated myocardial mass or vascular volume, can provide important additional functional information

beyond the anatomical information obtained during routine coronary arteriography.

A number of angiographic methods to assess coronary blood flow have previously been investigated [4–14]. However, the limitations of these techniques have hampered their eventual clinical implementation. We have previously used flow probes to validate an angiographic blood flow measurement technique based on the first pass distribution analysis, which addresses the previously reported limitations [15, 16]. In order to assess the severity of a stenosis using blood flow measurement at maximum hyperemia, it is necessary to estimate the expected normal hyperemic blood flow in the absence of a stenosis. In other words, it is necessary to assess whether the measured blood flow through a particular artery at maximum hyperemia is normal for its perfusion bed size. In the case of flow measurement using positron emission tomography (PET), the measured flow is normalized by the myocardial mass (ml/min/100 g of tissue). It is not possible to directly measure regional myocardial mass with angiography. However, it is possible to measure the dependent arterial lumen volume using densitometry [17], which can also be related to the myocardial mass [18, 19]. It is also possible to measure the sum of the arterial branch lengths using 3-D reconstruction of biplane images [20–22] and computed tomography (CT) [18, 19], which has been shown to be related to myocardial mass.

Fractional flow reserve (FFR), a parameter frequently used for identifying hemodynamically significant stenosis, is defined as the ratio of the maximal coronary flow through a stenotic vessel to the theoretical maximal coronary flow through the same vessel without a stenosis. It can potentially be determined using angiographic image data by measuring the maximum coronary blood flow through a stenotic vessel [15, 16, 23] and using the measured crown lumen volume [17] to predict the theoretical maximal coronary flow without a stenosis. We have previously shown in a simulation study that coronary blood flow can be estimated using the dependent arterial lumen volume and branch lengths [24]. This study presents an in vivo validation of this technique used to estimate hyperemic blood flow based on the dependent arterial lumen volume and branch lengths. Hyperemic blood flow in the absence of a stenosis was estimated using the angiographically measured dependent lumen volume in a swine animal model. Knowledge about the theoretical hyperemic blood flow can potentially be used to assess stenosis severity by quantifying FFR in the cardiac catheterization laboratory using only angiographic image data.

Methods

Animal preparation

The University of California–Irvine's Institutional Animal Care and Use Committee (IACUC) approved the procedures used in this study. Fasted swine (Yorkshire, 25–35 kg, $N = 10$) were sedated with xylazine (2.0 mg/kg), ketamine (10 mg/kg), and atropine (0.05 mg/kg). The animals were anesthetized with isoflurane (1–2%) and ventilated with 100% O_2. Ventilator settings were adjusted during the experiments to maintain Po_2 and Pco_2 within normal ranges. A peripheral vein was used for administrating medication and intravenous fluid. Arterial pressure was measured in the left carotid artery using a calibrated pressure transducer (TSD104A, Biopac Systems, Inc. Santa Barbara, CA). Carotid artery and jugular vein cut-downs were employed for sheath placement. Prior to catheterization, a 10,000 unit bolus of heparin was given. This was followed by additional 4,000–5,000 units per hour. The left main ostium was cannulated with a 6–7F hockey-stick catheter through the left carotid artery under fluoroscopic guidance. Electrocardiogram (ECG), femoral artery blood pressure and X-ray tube voltage (kVp) were continuously recorded (MP100, Biopac Systems, Inc. Santa Barbara, CA).

Each swine was positioned on its right side under a flat panel detector. The projection angle was optimized for separating the left anterior descending (LAD) and left circumflex (LCX) coronary artery perfusion beds. Intracoronary injection of papaverine (5–10 mg) was used to induce maximum hyperemia. For each animal, the papaverine dose was adjusted to determine the dose beyond which there was no additional increase in flow. Coronary angiograms were acquired within 90 s after intracoronary administration of papaverine. Hemodynamic data for all the pigs are shown in Table 1 where the mean and standard deviation (σ) of each parameter is also shown.

Prior to coronary angiography, pancuronium (0.1 mg/kg) was given intravenously. The ventilator was turned off at the end of a full expiration to minimize respiratory motion. A total of 10 ml of contrast material (Omnipaque-350; Princeton, NJ) was power injected (Leibel-Flarsheim Angiomat 6000; Cincinnati, OH) at 4 ml/s. An image of a calibration phantom positioned over the heart was also acquired to determine the correlation between image gray level and iodine mass. All images were acquired using a conventional X-ray tube (Dynamax 79-45/120, Machlett Laboratories, Stamford CT), a constant potential X-ray generator (Optimus M200, Philips Medical Systems, Shelton, CT) and a CsI amorphous-Si digital flat-panel detector (PaxScan 4030A, Varian Medical Systems).

After completing the angiographic part of the study in 3 swine, a midline sternotomy was performed. An incision was made in the pericardium, and the heart was supported with a pericardial cradle. The animal was heavily anesthetized, while the heart was arrested with a saturated KCl solution given through a jugular vein. The heart was then excised with the ascending aorta clamped to keep air bubbles out of the coronary vessels. The right coronary artery (RCA), LAD and LCX arteries were cannulated under saline to avoid air bubbles. A cast of the coronary arteries was prepared in the 3 hearts as described previously [17]. Briefly, Microfil (Canton Bio-Medical, Boulder, Colorado) was used to make a solid cast of the coronary vasculature. Cab-O-Sil (3% by weight, Eastman Kodak) was added to the Microfil to stop the flow in the coronary arterial-arteriolar vessels [17]. A freshly catalyzed (6% stannous 2-ethylhexoate and 3% ethyl silicate) solution of Microfil and Cab-O-Sil was perfused through the major coronary arteries (RCA, LAD and LCX arteries) and maintained at a pressure of 100 mmHg until the solution hardened after approximately 40 min.

Table 1 Hemodynamic data for all animals showing the mean and standard deviation (σ) of each parameter

	Mean	σ
Body weight (kg)	31	4
P_a (mmHg)	56.0	10.9
ΔP with papaverine (%)	26.9	9.7
Heart rate (beats/min)	93.1	10.5

Stem flow-crown size relationship

Various possible theoretical explanations for the coronary arterial tree design include the principles of minimum work [25, 26], optimal design [27], minimum blood volume [28] and minimum total shear force on the vessel wall [29]. Irrespective of the underlying design principles, previous studies have observed relationships between coronary blood flow (Q) and oxygen consumption or metabolic need [30]; coronary blood flow and myocardial mass (M) [31]; and myocardial mass and the cumulative arterial branch lengths (L) or crown lumen volume (V) that supply it [20, 21]. In investigating the design of the coronary arterial system, the coronary arterial tree can be recursively decomposed into stem and crown subunits, where a stem is defined as any segment between two consecutive bifurcation (or trifurcation) points, and the corresponding crown is defined as a collection of all the branches distal to the stem whose terminals consist of the same diameter (see Fig. 1). Using this decomposition of the coronary arterial tree, previous reports have shown the following relationships [22, 24, 32]:

$$Q = k_L L \tag{1}$$

$$L = k_{LV}\left(\frac{V}{V_{ref}}\right)^{3/4} \tag{2}$$

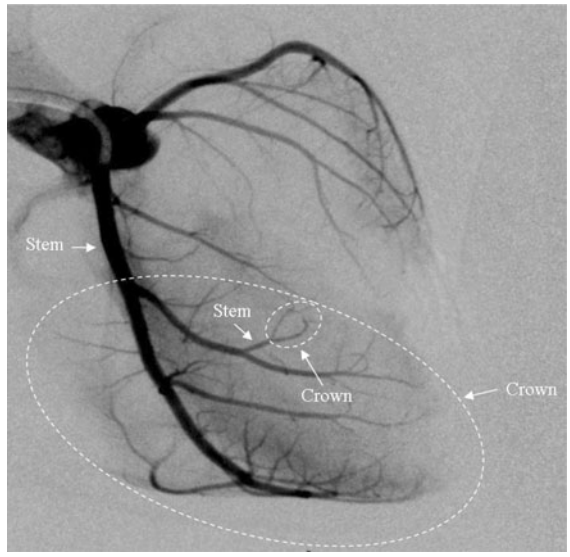

Fig. 1 A coronary angiogram showing the definition of stems and crowns

$$Q = k_V \left(\frac{V}{V_{ref}} \right)^{3/4} \quad (3)$$

Applying the principle of minimum energy to the design of the coronary arterial system allowed a linear relationship between blood flow through a stem and the corresponding crown length to be predicted (see Eq. 1) [22, 32]. A power law relationship was also predicted between the crown volume and length (see Eq. 2). Combining Eqs. 1 and 2 yield the relationship between Q and V that is expressed in Eq. 3. In Eqs. 1–3, k_L, k_{LV} and k_V are the scaling coefficients and V_{ref} is a reference volume in order to make V raised to the power of ¾ unitless.

When compared with Kleiber's allometry [33], which relates metabolic rate to body mass raised to an exponent of 3/4, Eq. 3 is consistent with this 3/4 allometry law given that metabolic rate scales with coronary blood flow [30] and that mass scales with total blood volume [19, 31, 34]. Therefore the following relationship can be used to relate coronary blood flow with the dependent myocardial mass (M):

$$Q = k_M \left(\frac{M}{M_{ref}} \right)^{3/4} \quad (4)$$

In Eq. 4, k_M is the scaling coefficients and M_{ref} is a reference volume in order to make M raised to the power of ¾ unitless.

Techniques to measure coronary lumen volume, flow and arterial length will be described next.

Regional lumen volume measurement

Coronary artery lumen volume can be measured using densitometry [17]. System calibration is required to quantify the iodine mass from the densitometry signal [15, 35]. An iodine calibration phantom, containing known amounts of iodine, was imaged over the heart region of each swine. The calibration phantom consisted of a series of rods each containing contrast material with diameters ranging from 0.76 to 3.35 mm and iodine masses ranging from 7.66 to 112.04 mg (see Fig. 2a). The iodine concentration in the calibration phantom was approximately the same as the undiluted contrast material (350 mg/ml). Correction for the magnification difference between the coronary arteries and the calibration phantom was performed by accounting for their distances from the X-ray source. After logarithmic transformation followed by phase-matched subtraction, the integrated gray level (G) inside the region of interest (ROI) was directly converted to arterial volume using the following equation:

$$V = G\frac{F_M}{C} \quad (5)$$

where F_M is the integrated gray level to iodine mass conversion factor, and C is the iodine concentration of the bolus entering the arteries of interest. The iodine concentration inside the opacified arteries was assumed to be the same as that of the injected contrast material. This assumption stems from the protocol where contrast material was injected at a rate in which it completely replaces blood entering the coronary arteries [15, 16]. Using the acquired image of the calibration phantom, F_M was determined from the

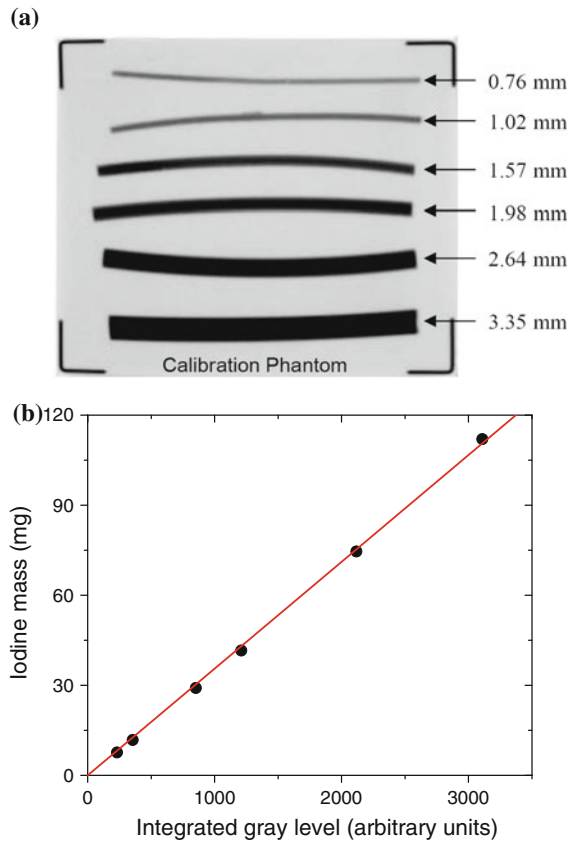

Fig. 2 Image of the calibration phantom is shown (**a**) along with an example of a calibration curve showing the relationship between iodine mass (mg) and measured integrated gray levels (**b**)

slope ($\Delta M/\Delta G$) of the regression line that correlates the known iodine masses (M) with the measured integrated gray levels (G) (see Fig. 2b). A correction for the magnification differences between the heart and the calibration phantom placed on the pig's thorax was also required. The expression for F_M is

$$F_M = \frac{\Delta M D_H^2}{\Delta G D_C^2}, \quad (6)$$

where D_H is the X-ray source-to-heart distance and D_C is the source-to-calibration distance. D_C was determined from an image of the 4 markers on the calibration phantom. D_H was assumed to be less than D_C by 5 cm, which was the approximate distance from the heart to the sternum and the left side of the chest wall.

Regional lumen volume measurements were made by drawing different arterial ROIs corresponding to arterial segments between bifurcation points on the main trunk of the LAD coronary artery. Figure 3 shows an example of the arterial ROI superimposed over the LAD coronary artery. The arterial tree was divided into 1–6 segments where the branches with visible overlap were not used. Regional lumen volume measurements were made from the 6 different crowns. The regional volume measurements were made down to an arterial diameter of $\sim$0.5 mm, which is close to the limiting spatial resolution of the angiographic system. This required an ROI around the visible arterial tree so the effect of the myocardial blush on the densitometry signal and the calculated arterial lumen volume was minimal. The in vivo validation of the technique to measure arterial lumen volume using coronary arteriography has previously been reported [17].

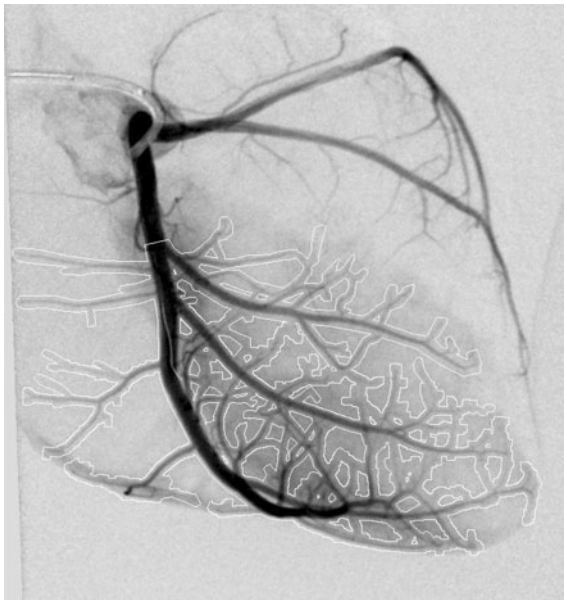

Fig. 3 Coronary angiogram with an arterial ROI superimposed over the LAD coronary artery for lumen volume measurement

Regional blood flow measurement

Flow measurements were made using a first pass analysis technique, which models the arterial volume compartment supplied by a major coronary artery as a reservoir with a single input. The model does not require any assumptions regarding the internal structure of the arterial volume compartment or the nature of the exit conduits. Instead, the necessary assumptions are that (1) the flow measurement is performed before the contrast material begins to exit the volume compartment (which includes microvessels) and (2) the input contrast concentration is known during the flow measurement period. Figure 4 shows a coronary arteriogram with a global ROI used for blood flow measurement. A global ROI, which includes the myocardial blush, is particularly important for flow measurement at hyperemia where the transit time within the epicardial arteries is relatively short. An arterial ROI (see Fig. 3) is adequate for flow measurement at baseline but will underestimate the flow at hyperemia.

The measured volume difference (ΔV_a) and the known time between subsequent images (Δt) were used to calculate absolute volumetric blood flow:

$$Q = \Delta V_a / \Delta t \quad (7)$$

The in vivo validation of the coronary blood flow measurement technique using a transit time flow probe has previously been reported [15, 16, 23].

Regional arterial length measurement

The casted hearts were imaged using a cone-beam computed tomography (CT) system to measure arterial length. The cone-beam CT system was implemented using a CsI amorphous-Si digital flat-panel detector (PaxScan 4030A, Varian Medical Systems), a high precision motor (Kollmorgen Goldline direct drive rotary), and a conventional X-ray tube (0.6 and 1.2 mm focal spot sizes). The entire system was

Fig. 4 Coronary angiogram with a global ROI superimposed over the LAD coronary artery for blood flow measurement

mounted on an optical bench. The flat panel has a total available coverage of 40 × 30 cm and a pixel size of 194 × 194 μm. The reconstruction voxel size was 200 × 200 × 200 μm^3. The casted hearts were then placed on a rotating platform and 180 dual-energy projections were acquired. Dual-energy subtraction was applied to suppress tissue contrast and isolate blood vessel features. Images were reconstructed with commercially available software designed for cone-beam reconstruction using a modified Feldkam algorithm (Exxim COBRA). The reconstructed CT volumes have a dimension of 515 × 512 × 512 voxels, where each voxel is encoded by 16 bits.

After acquiring and reconstructing the images, numerous post-acquisition image processing techniques were used to determine crown length [18, 19]. Briefly, the process begins with differentiating between voxels belonging to the myocardium versus those belonging to the arterial branches. The extracted arterial voxels were then used to determine crown volume. The extracted arterial branches were then thinned until only their skeletal centerlines remained. These centerlines were used to calculate crown length [18, 19]. In order to ensure there was a uniform terminal diameter vessel, segments with diameters smaller than 0.7 mm were removed. An example of the 3-D reconstructed coronary arteries is shown in Fig. 5.

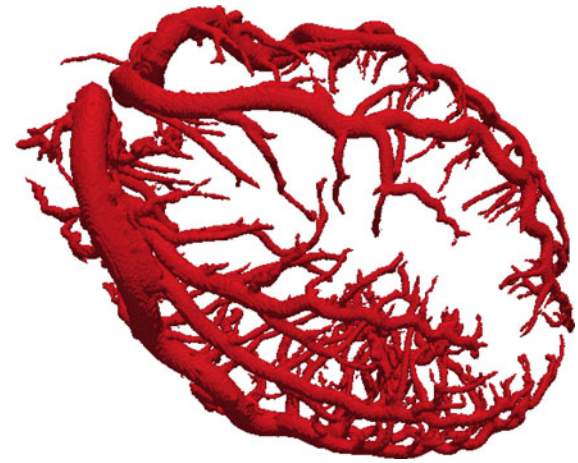

Fig. 5 3-D reconstruction of coronary arteries using cone-beam CT data from a casted heart

Results

Stem flow-crown volume relationship

Figure 6 shows the relationship between stem hyperemic flow and the corresponding crown lumen volume using densitometry. The stem hyperemic flow (Q) and the associated crown lumen volume (V) were related by $Q = 115.2\ V^{3/4}$ ($r = 0.97$, SEE = 10.2 ml/min, $N = 33$). The standard error of estimate (SEE) of the regression line was calculated to be 10.2 ml/min. Figure 7 shows the relationship between stem hyperemic flow and the corresponding crown lumen volume where hyperemic blood flow was measured using densitometry and lumen volume was measured using cone-beam CT data. The stem hyperemic flow and the associated crown lumen volume were related by $Q = 109.3\ V^{3/4}$ ($r = 0.99$, SEE = 7.3 ml/min, $N = 18$). These results are in agreement with the prediction from Eq. 3. Table 2 shows the stem hyperemic blood flow, angiographic crown lumen volume, CT crown lumen volume and CT crown arterial length for the different animals and selected crowns.

Stem flow-crown length relationship

Figure 8 shows the relationship between stem hyperemic flow measured using densitometry and the corresponding crown length measured using cone-beam CT. The stem hyperemic flow and the associated crown length (L) were related by $Q = 2.2\ L$

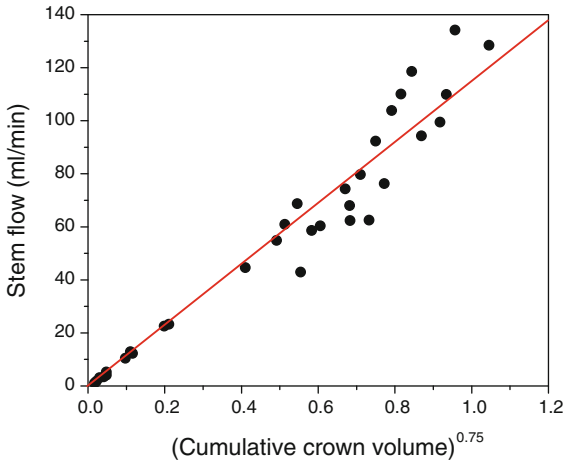

Fig. 6 Correlation of stem hyperemic blood flow and normalized crown lumen volume raised to the power of ¾. Densitometry was used to measure both blood flow and lumen volume. All crown volumes were normalized to a crown lumen volume of 1 ml (V_{ref} = 1 ml, see Eq. 3)

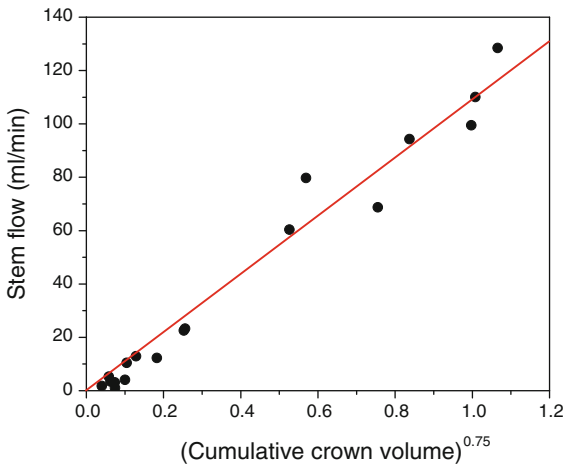

Fig. 7 Correlation of stem hyperemic blood flow and normalized crown lumen raised to the power of ¾. Densitometry was used to measure blood flow and cone-beam CT was used to measure lumen volume. All crown volumes were normalized to a crown lumen volume of 1 ml (V_{ref} = 1 ml, see Eq. 3)

(r = 0.99, SEE = 5.5 ml/min, N = 18). This result is in agreement with the prediction from Eq. 1.

Discussions

There have been significant advances in the ability to assess myocardial blood flow using radionuclide imaging techniques. Conventional single photon perfusion imaging techniques that use either a planar or a single photon emission computed tomography (SPECT) permits only relative measurement of regional blood flow under stress conditions or at rest. However, these techniques cannot quantify the absolute myocardial perfusion. Previous studies have

Table 2 Stem hyperemic blood flow, angiographic crown lumen volume ($Volume_{angio}$), CT crown lumen volume ($Volume_{CT}$) and CT crown arterial length ($Length_{CT}$) for different selected crowns are shown for all the animals

Animal	Flow (ml/min)	$Volume_{Angio}$ (ml)	$Volume_{CT}$ (ml)	$Length_{CT}$ (cm)
1	125.4	0.65	1.01	45.6
1	84.3	0.38	0.69	34.7
1	27.4	0.10	0.16	7.3
1	15.3	0.05	0.10	5.8
1	7.3	0.02	0.02	2.3
1	4.1	0.01	0.03	2.0
1	1.6	0.004	0.03	1.3
2	133.5	0.92	1.00	51.1
2	103.5	0.66	0.47	34.1
2	79.2	0.53	0.43	30.8
2	22.7	0.06	0.07	6.0
2	4.7	0.02	0.03	2.4
3	182.1	1.1	1.09	56.3
3	136.0	0.87	0.79	43.4
3	34.8	0.13	0.16	9.0
3	16.4	0.05	0.05	3.8
3	6.2	0.02	0.05	2.4
3	3.4	0.007	0.01	1.4
4	132.2	0.79		
4	101.9	0.66		
4	93.4	0.59		
5	100.1	0.59		
5	86.7	0.49		
6	162.8	0.93		
6	158.6	0.81		
6	120.6	0.71		
7	154.1	0.85		
8	123.1	0.59		
9	110.0	0.69		
9	74.9	0.49		
10	119.4	0.59		
10	95.4	0.42		
10	73.3	0.31		

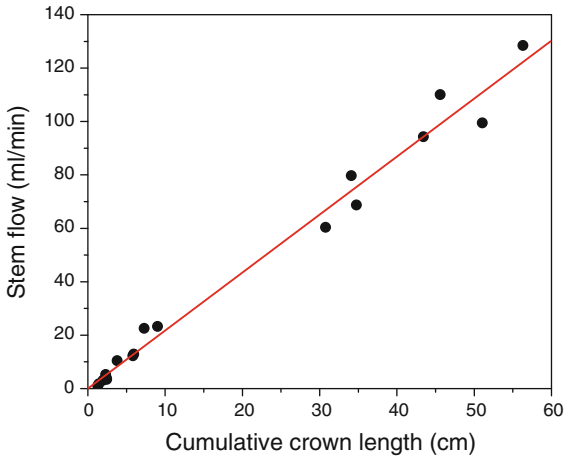

Fig. 8 Correlation of stem hyperemic blood flow and crown branch lengths. Densitometry was used to measure blood flow and cone-beam CT was used to measure branch lengths

described [36, 37] a method for quantifying absolute regional myocardial perfusion after intravenous injection of nitrogen-13 (N-13) ammonia and rapid sequential imaging by positron emission tomography (PET). Although PET offers unique clinical capabilities such as assessment of myocardial viability and perfusion, in this era of cost containment it is difficult to predict the rapid growth of such a complex and expensive technology. It seems more likely that PET will continue to be primarily an investigative tool.

There have been developments in other imaging modalities such as magnetic resonance imaging (MRI), computed tomography (CT) and echocardiography in efforts to develop a noninvasive screening technique to assess myocardial perfusion. MRI is capable of detecting indicators of coronary blood flow in large vessels and myocardium using FLASH sequence techniques. CT has also been used for assessing myocardial perfusion after intravenous injection of contrast material. Echocardiography, after intravenous injection of microbubble contrast agent, is another noninvasive imaging modality that has been used to quantify myocardial perfusion. However, these alternative methods pose significant challenges and require further development to be clinically useful [38].

The previously mentioned modalities are focused on the important problem of developing a noninvasive screening technique to assess coronary artery disease (CAD). However, it is of paramount importance to accurately assess the severity of coronary artery stenosis after a patient has been referred to the cardiac catheterization laboratory. This is especially true in the case of an intermediate coronary lesion where coronary arteriography cannot determine whether the lesion caused the ischemia.

FFR, developed by Pijls et al., was introduced to provide a physiological measurement of coronary stenosis in the cardiac catheterization laboratory. FFR is defined as a percentage of normal hyperemic flow transmitted across the stenotic artery. FFR can be derived by dividing the pressure distal to the stenosis by the aortic pressure. The distal pressure is measured by using a pressure-sensing wire that has been advanced across the stenosis during cardiac catheterization. Aortic pressure is simultaneously measured at the catheter tip with a fluid filled pressure transducer. Theoretically, a FFR value of 0.6 means the maximum myocardial flow across the stenosis is only 60% of what it should be without the stenosis. Likewise, a FFR of 0.9 after coronary intervention means that the maximum flow to the myocardium is 90% of a completely normal vessel.

The concept of fractional flow reserve has been thoroughly examined by both experimental and clinical studies [39–41]. A non-ischemic threshold value range of 0.75–0.80 has been prospectively confirmed [39] and was compared to the non-invasive stress testing [41, 42]. A FFR < 0.75 was associated with inducible ischemia (specificity, 100%), whereas a value >0.80 indicated an absence of inducible ischemia in the majority of patients (sensitivity, 90%). Although FFR is clinically reliable and useful, its application requires inserting an angioplasty sensor guide wire across the stenotic lesion and the potential risks that entails. Therefore, it would be important if angiographic image data could be used instead to measure coronary blood flow and FFR because it eliminates those risks.

Early densitometry techniques to measure coronary artery cross-sectional area and blood flow using angiographic image data were hampered by physical and physiological limitations. The primary physical limitation was the non-linearity in the image intensifier television-based imaging chain. Early studies using densitometry produced disappointing results because no corrections were made for this. The major cause of this non-linearity is the physical degradation factors that include X-ray scatter and veiling glare [35]. Currently, there are techniques available to correct for the X-ray scatter and veiling glare

[43, 44]. These techniques can be used to address this major physical limitation. Furthermore, new generations of flat panel detectors have substantially improved the capability for quantitative analysis. The veiling glare has been substantially reduced and the pincushion distortion has been eliminated.

A physiological limitation for measuring coronary artery blood flow and lumen volume has been the unknown blood iodine concentration. We have shown that power injection of contrast material can produce an undiluted bolus of contrast in the arterial tree. Therefore, the iodine concentration can be assumed to be the same as the injected contrast material [15, 16]. By addressing the physical and physiological limitations, it is now possible to accurately measure coronary blood flow and lumen volume using densitometry [16, 17, 23].

A previously reported densitometry technique [16] can be used to measure the maximum hyperemic coronary blood flow through a stenotic artery. However, the reduction of hyperemic blood flow due to the stenosis is not known. Previous studies have shown a linear relationship amongst lumen volume, arterial branch lengths and the associated myocardial mass [18–21]. A previously reported simulation study has also shown that coronary blood flow can be estimated using the dependent arterial lumen volume or branch lengths [24]. In this study, the correlation between densitometry measured stem hyperemic flow (Q) and crown lumen volume (V) for LAD shows (see Eq. 3) a linear relationship between Q and $V^{3/4}$ (see Fig. 6). In densitometry, hyperemic blood flow and crown lumen volume are measured using the same image data. In order to eliminate the potential possibility of correlated errors between densitometry derived lumen volume and hyperemic blood flow, the measured hyperemic blood flow was also correlated with CT derived lumen volume (see Fig. 7). This was done for the three animals where CT data was available from the casted hearts. The results indicated that there is a linear correlation between hyperemic blood flow and lumen volume regardless of the method used for lumen volume measurement.

The results of the correlation between stem hyperemic flow and crown arterial lengths (L) (see Eq. 1) show a linear relationship between Q and L (see Fig. 8). Likewise, these correlations were done for the three animals where CT data was available from casted hearts.

The results from the current animal study agree with our previous simulation results [24], indicating that crown lumen volume and branch lengths can be used to estimate the expected normal hyperemic blood flow in the absence of a stenosis (see Figs. 6, 7, 8). It is also possible to measure crown lumen volume [17] and crown branch length [22] using coronary angiography. Crown lumen volume can be easily measured using the same single plane angiography images used for volumetric blood flow measurement [15, 16, 23]. Lumen volume can be measured using an arterial ROI (see Fig. 3). This process can potentially be automated to make the lumen volume measurement available immediately after image acquisition. On the other hand, crown branch length measurement requires biplane image acquisition and 3-D reconstruction of the biplane images [22]. It also requires that the terminal vessels have uniform diameters. Therefore, the measured crown lengths using imaging modalities with different spatial resolutions, such as angiography and CT, can be different. Currently, the available 3-D reconstruction algorithms of biplane images are time consuming. Furthermore, it might be necessary to image the arterial tree in more than two projections to overcome the limitations manifested by vessel overlap [45]. Therefore, it is expected that crown lumen volume can potentially be more feasible for clinical implementation.

Regional lumen volume and arterial branch lengths were measured using casted hearts and cone-beam CT (see Figs. 7, 8). It is also potentially possible to measure these parameters using CT angiography, since the image quality for this emerging technology has been improving. This will make it possible to estimate an expected hyperemic blood flow along the coronary artery tree. The measured distal crown lumen volume or branch lengths can alternatively be used to estimate the regional myocardial mass at risk since these parameters are interdependent [18–21].

Clinical implications and limitations

The clinical application of our technique has some potential limitations. One potential limitation is that flow measurements have to be made before contrast material starts exiting the vascular bed. Also, diluted contrast material cannot enter the vascular bed during this time interval. However, since all the flow

measurements in this study were made during the first two cardiac cycles after the start of contrast injection, it indicates that the LAD vascular bed empties out slowly enough to allow for the flow measurements to be performed.

Another potential limitation is the overlapping of vascular beds from multiple vessels. This problem is an inherent limitation of the projection nature of radiographic images. However, it is possible to choose an imaging projection that will minimize potential errors.

This flow measurement technique has not been tested when there is collateral blood flow present. However, clinically, the situations most likely to involve collateral flow are those in which lesion severity has been reliably assessed by angiography (e.g. >90%). For less severe stenosis in which angiographic assessment is less reliable, the frequency of appreciable collateral flow is markedly reduced.

Our current implementation of this technique utilizes phase-matched time subtraction images during a breath hold. The flow measurements can be completed in approximately two cardiac cycles. This reduces the possibility of motion misregistration artifacts in comparison to other techniques that require temporal subtraction images during $\sim$15–20 heart beats [46]. However, it is necessary to minimize potential misregistration artifacts during image acquisition. This requirement is similar to other imaging modalities such as CT and MRI. Results from a previous simulation [24] and this study have both shown that a relationship exists between hyperemic blood flow and crown lumen volume. A previous report has shown that crown lumen volume can be measured using single plane angiographic images [17]. The results from this study show that the measured crown lumen volume can be used to predict the theoretical hyperemic blood flow into an arterial tree of interest. Knowledge of this theoretical hyperemic blood flow can potentially be used to assess stenosis severity by quantifying FFR in the cardiac catheterization laboratory. FFR can potentially be determined using angiographic image data by measuring the hyperemic coronary blood flow through a stenotic vessel and using the measured crown lumen volume to predict the theoretical hyperemic blood flow without a stenosis. Therefore, angiographic images can be used to assess both anatomic and hemodynamic significance of a stenosis.

Acknowledgments This research is supported in part by Grant R01 HL89941 awarded by the NHLBI, DHHS.

Conflict of interest None.

References

1. Detre KM, Wright E, Murphy ML, Takaro T (1975) Observer agreement in evaluating coronary angiograms. Circulation 52:979–986
2. Zir LM, Miller SW, Dinsmore RE, Gilbert JP, Hawthorne JW (1976) Interobserver variability in coronary angiography. Circulation 53:627–632
3. DeRouen TA, Murray JA, Owen W (1977) Variability in the analysis of coronary arteriogram. Circulation 55: 324–328
4. Rutishauser W, Bussman WD, Noseda G, Meier W, Wellauer J (1970) Blood flow measurement through single coronary arteries by Roentgen densitometry. Am J Roentgenol 109:12–20
5. Smith HC, Sturm RE, Wood EH (1973) Videodensitometric system for measurement of vessel blood flow, particularly in the coronary arteries in man. Am J Cardiol 32:144–150
6. Foerster JM, Lantz BM, Holcroft JW, Link DP, Mason DT (1981) Angiographic measurement of coronary blood flow by videodilution technique. Acta Radiologica Diagn 22:121–127
7. Foerster JM, Link DP, Lantz BM, Lee G, Holcroft JW, Mason DT (1981) Measurement of coronary reactive hyperemia during clinical angiography by videodilution technique. Acta Radiologica Diagn 22:209–216
8. Bursch JH (1983) Use of digitized functional angiography to evaluate arterial blood flow. Cardiovasc Inter Radiol 6:303–310
9. Hodgson JM, LeGrand V, Bates ER et al (1985) Validation in dogs of a rapid digital angiographic technique to measure relative coronary blood flow during routine cardiac catheterization. Am J Cardiol 55:188–193
10. Vogel RA (1985) The radiographic assessment of coronary blood flow parameters. Circulation 72:460–465
11. Eigler NL, Pfaff JM, Zeiher A, Whiting JS, Forrester JS (1989) Digital angiographic impulse response analysis of regional myocardial perfusion: linearity, reproducibility, accuracy and comparison with conventional indicator dilution curve parameters in phantom and canine models. Cir Res 64:853–866
12. Marinus H, Buis B, van Benthem A (1990) Pulsatile coronary flow determination by digital angiography. Int J Cardiac Imaging 5:173–182
13. Pijls NH, Uijen GJ, Hoevelaken A et al (1990) Mean transit time for the assessment of myocardial perfusion by videodensitometry. Circulation 81:1331–1340

14. Hangiandreou N, Folts J, Peppler W, Mistretta C (1991) Coronary blood flow measurement using an angiographic first pass distribution technique: a feasibility study. Med Phys 18:947–954
15. Molloi S, Bednarz G, Tang J, Zhou Y, Mathur T (1998) Absolute volumetric coronary blood flow measurement with digital subtraction angiography. Int J Cardiac Imaging 14:137–145
16. Molloi S, Zhou Y, Kassab GS (2004) Regional volumetric coronary blood flow measurement by digital angiography: in vivo validation. Acad Radiol 11:757–766
17. Molloi S, Kassab GS, Zhou Y (2001) Quantification of coronary artery lumen volume by digital angiography: in vivo validation. Circulation 104:2351–2357
18. Le H, Wong JT, Molloi S (2008) Estimation of regional myocardial mass at risk based on distal arterial lumen volume and length using 3D micro-CT images. Comput Med Imaging Graph 32:488–501
19. Le HQ, Wong JT, Molloi S (2008) Allometric scaling in the coronary arterial system. Int J Cardiovasc Imaging 24:771–781
20. Seiler C, Kirkeeide RL, Gould KL (1992) Basic structure-function relations of the coronary vascular tree. The basis of quantitative coronary arteriography for diffuse coronary artery disease. Circulation 85:1987–2003
21. Seiler C, Kirkeeide RL, Gould KL (1993) Measurement from arteriograms of regional myocardial bed size distal to any point in the coronary vascular tree for assessing anatomic area at risk. J Am College Cardiol 21:783–797
22. Zhou Y, Kassab GS, Molloi S (2002) In vivo validation of the design rules of the coronary arteries and their application in the assessment of diffuse disease. Phys Med Biol 47:977–993
23. Molloi S, Ersahin A, Tang J, Hicks J, Leung CY (1996) Quantification of volumetric coronary blood flow with dual-energy digital subtraction angiography. Circulation 93:1919–1927
24. Molloi S, Wong JT (2007) Regional blood flow analysis and its relationship with arterial branch lengths and lumen volume in the coronary arterial tree. Phys Med Biol 52:1495–1503
25. Murray CD (1926) The physiological principle of minimum work applied to the angle of branching of arteries. J Gen Physiol 9:835–841
26. Murray CD (1926) The physiological principle of minimum work. I. The vascular system and the cost of blood volume. Proc Natl Acad Sci USA 12:207–214
27. Rosen R (1967) Optimality principles in biology
28. Kamiya A, Togawa T (1972) Optimal branching structure of the vascular tree. Bull Math Biophys 34:431–438
29. Zamir M (1976) Role of shear forces in arterial branching. J Gen Physiol 67:213–222
30. Alella A, Williams FL, Bolene-Williams C, Katz LN (1955) Interrelation between cardiac oxygen consumption and coronary blood flow. Am J Physiol 183:570–582
31. Choy JS, Kassab GS (2008) Scaling of myocardial mass to flow and morphometry of coronary arteries. J Appl Physiol 104:1281–1286
32. Zhou Y, Kassab GS, Molloi S (1999) On the design of the coronary arterial tree: a generalization of Murray's law. Phys Med Biol 44:2929–2945
33. Kleiber M (1932) Body size and metabolism. Hilgardia 6:315–353
34. Prothero JW (1980) Scaling of blood parameters in mammals. Comp Biochem Physiol Part A Physiol 67:649–657
35. Molloi SY, Mistretta CA (1989) Quantification techniques for dual-energy cardiac imaging. Med Phys 16:209–217
36. Di Carli M, Czernin J, Hoh CK et al (1995) Relation among stenosis severity, myocardial blood flow, and flow reserve in patients with coronary artery disease. Circulation 91:1944–1951
37. Nagamachi S, Czernin J, Kim AS et al (1996) Reproducibility of measurements of regional resting and hyperemic myocardial blood flow assessed with PET. J Nucl Med 37:1626–1631
38. Rutishauser W (1999) The Denolin lecture 1998. Towards measurement of coronary blood flow in patients and its alteration by interventions. Eur Heart J 20:1076–1083
39. Pijls NH, De Bruyne B, Peels K et al (1996) Measurement of fractional flow reserve to assess the functional severity of coronary-artery stenoses. N Engl J Med 334:1703–1708
40. De Bruyne B, Bartunek J, Sys SU, Pijls NH, Heyndrickx GR, Wijns W (1996) Simultaneous coronary pressure and flow velocity measurements in humans. Feasibility, reproducibility, and hemodynamic dependence of coronary flow velocity reserve, hyperemic flow versus pressure slope index, and fractional flow reserve. Circulation 94:1842–1849
41. De Bruyne B, Bartunek J, Sys SU, Heyndrickx GR (1995) Relation between myocardial fractional flow reserve calculated from coronary pressure measurements and exercise-induced myocardial ischemia. Circulation 92:39–46
42. Kern MJ (2000) Coronary physiology revisited: practical insights from the cardiac catheterization laboratory. Circulation 101:1344–1351
43. Ersahin A, Molloi S, Yao-Jin Q (1995) A digital filtration technique for scatter-glare correction based on thickness estimation. IEEE Trans Med Imaging 14:587–595
44. Zhou Y, Mathur T, Molloi S (1999) Scatter and veiling glare estimation based on sampled primary intensity. Med Phys 26:2301–2310
45. Wu J, Parker DL (1990) Three-dimensional reconstruction of coronary arteries using more than two projections. In: Loew MH (ed) Medical imaging IV: image processing. SPIE, Bellingham, pp 77–84
46. Pijls NH, Uijen GJ, Hoevelaken A et al (1990) Mean transit time for videodensitometric assessment of myocardial perfusion and the concept of maximal flow ratio: a validation study in the intact dog and a pilot study in man. Int J Card Imaging 5:191–202